# A response spectrum method for peak floor acceleration demands in earthquake excited structures

Lukas Moschen[a,*], Christoph Adam[a], Dimitrios Vamvatsikos[b]

[a] *Unit of Applied Mechanics, University of Innsbruck, 6020 Innsbruck, Austria*
[b] *School of Civil Engineering, National Technical University of Athens, Greece*

**Abstract**

This paper addresses the prediction of the median peak floor acceleration (PFA) demand of elastic structures subjected to seismic excitation by means of an adapted response spectrum method. Modal combination is based on a complete quadratic combination (CQC) rule. In contrast to previous studies, in the present contribution closed form solutions for the correlation coefficients and peak factors entering the CQC rule are derived using concepts of normal stationary random vibration theory. A ground motion set, which matches the design response spectrum for a specific site and a target dispersion, is used to define the stochastic base excitation. The response spectrum method is tested for various planar and spatial generic high-rise structures subjected to this particular ground motion set. A comparison of the outcomes with the results of computationally more expensive response history analyses shows the applicability and accuracy of the proposed simplified method.

*Keywords:* CQC rule, peak factor, peak floor acceleration demand, random vibration theory, response spectrum method, seismic excitation

## 1. Introduction

A modal combination procedure is presented aiming at assessing the median peak floor acceleration (PFA) response of elastic structures subjected to normal stationary base excitation. In order to avoid computationally expensive procedures such as response history analysis (RHA), the latest seismic codes and guidelines provide the engineering community with simplified approaches. For instance, the FEMA P-58-1 document [1] proposes methods to estimate the statistical distribution of the PFA demand even for inelastic structures. Based on the type of lateral load bearing structure (moment resisting frame, braced frame, or structural wall) different coefficients rule the handling of the mathematical framework. Another possibility is to use the method of the nonstructural components (NSCs) chapter of the U.S. standard ASCE 7-10 [2]. Here, the ratio between the seismic design force and the mass of the NSC delivers an estimate of the median PFA demand, implying that the NSC is rigid. The bottom line is that these simplified procedures are adequate for a quick pre-design, however, lack generality in application.

In many cases a more sophisticated procedure is required to estimate the PFA demand, because, in general, load bearing structures have a three dimensional setup and may exhibit irregularities to fulfill the functionality and architectural design of a building. Based on a parametric study of both elastic and inelastic structures, Chaudhuri and Hutchinson [3, 4] recommended empirical equations and a modified square-root-of-the-sum-of-the-squares (SRSS) method to estimate the PFA demand. The SRSS modal combination rule originally developed by Rosenblueth et al. [5] provides a statistical combination of modal peak responses, and can be used for any relative response quantity such as relative displacements or internal forces. Accepting the

*Corresponding author
*Email address:* lukas.moschen@uibk.ac.at (Dimitrios Vamvatsikos)

assumptions of the stationary random vibration theory [6], Der Kiureghian derived the complete quadratic combination rule [7, 8], where additionally the correlation between modal *displacements* is considered. It is of great importance to note here that modal displacements are *relative* response quantities. In his further research the method is referred to as the CQC combination rule [9, 10]. Non-stationary stochastic processes are a more realistic representation of structural responses due to earthquake loading. Therefore, Cacciola et al. [11] developed a modal correction method, which is able to estimate first- and second-order statistics of relative response quantities due to stationary *and* non-stationary stochastic input. The numerical procedure introduced by Schenk et al. [12] can be used to estimate efficiently the second-order statistics of relative response quantities of structures responding linearly *and* non-linearly due to stationary *and* non-stationary stochastic input.

Recently, Taghavi and Miranda [13] and Taghavi [14] derived the *extended* CQC rule, which allows the prediction of the PFA demand in elastic structures by fitting the correlation coefficients and peak factors based on real ground motions recorded in earthquake events. Results of a pilot study by the authors of the present study revealed that the extended CQC method yields reasonable results for planar systems, however, for spatial structures with closely spaced natural frequencies a more robust formulation is required. Pozzi and Der Kiureghian [15] concluded from their assessment of the PFA response that modal acceleration combination according to the SRSS rule may lead to an incorrect prediction of the absolute acceleration. In their most recent paper [16] they presented a response spectrum method for PFA demands using the CQC rule and numerically derived correlation coefficients and peak factors.

The present contribution also provides a response spectrum method for PFA demands of elastic structures. In contrast to the latter study [16], closed form solutions of the correlation coefficients and peak factors for the CQC rule are derived rigorously based on normal stationary random vibration theory. In application examples the PFA demands of six-, twelve-, and 24-story planar as well as spatial generic structures are estimated, and the outcomes are set in contrast to results from RHA. The results demonstrate that the proposed method delivers an excellent prediction of the PFA response.

## 2. Modal response history analysis

Consider an elastic multi-degree-of-freedom (MDOF) frame structure subjected to a uniform base excitation $\ddot{u}_g(t)$. The coupled set of equations of motion for any instant in time reads as [17]

$$\mathbf{M}\ddot{\mathbf{u}}^{(rel)}(t) + \mathbf{C}\dot{\mathbf{u}}^{(rel)}(t) + \mathbf{K}\mathbf{u}^{(rel)}(t) = -\mathbf{M}\mathbf{e}\ddot{u}_g(t) \tag{1}$$

in which $\mathbf{M}$ denotes the mass matrix, $\mathbf{C}$ the damping matrix, and $\mathbf{K}$ the stiffness matrix of the structure. Vector $\mathbf{u}^{(rel)}(t)$ contains the $N$ relative deformations related to the $N$ dynamic degrees of freedom with respect to the motion of the ground. The right hand side of Equation (1) represents the forcing function in terms of inertia forces due to the base excitation $\ddot{u}_g(t)$. Its spatial distribution is governed by the quasi-static influence vector $\mathbf{e}$. Equation (1) describes the motion of a planar structure or of a spatial structure subjected to horizontal ground motion in one principal direction. The extension to base excitation in both horizontal principal directions is straight forward, however, for the sake of clarity not further pursued.

The vector of total acceleration, $\ddot{\mathbf{u}}(t) = \ddot{\mathbf{u}}^{(rel)}(t) + \mathbf{e}\ddot{u}_g(t)$, is modally expanded into the $N$ mode shapes $\phi_i$,$i = 1, ..., N$,

$$\ddot{\mathbf{u}}(t) = \sum_{i=1}^{N} \phi_i \Gamma_i \ddot{d}_i(t) = \sum_{i=1}^{N} \phi_i \Gamma_i \ddot{d}_i^{(rel)}(t) + \mathbf{e}\ddot{u}_g(t) = \sum_{i=1}^{N} \phi_i \Gamma_i \ddot{d}_i^{(rel)}(t) + \sum_{i=1}^{N} \phi_i \Gamma_i \ddot{u}_g(t) \tag{2}$$

where $\Gamma_i = \left(\phi_i^\intercal \mathbf{M}\mathbf{e}\right) / \left(\phi_i^\intercal \mathbf{M}\phi_i\right)$ is the generalized participation factor and $\ddot{d}_i(t) = \ddot{d}_i^{(rel)}(t) + \ddot{u}_g(t)$ the total acceleration of the $i$th modal coordinate. The modal coordinate $d_i^{(rel)}(t)$ is governed by the $i$th modal oscillator equation,

$$\ddot{d}_i^{(rel)}(t) + 2\zeta_i\omega_i\dot{d}_i^{(rel)}(t) + \omega_i^2 d_i^{(rel)}(t) = -\ddot{u}_g(t) \tag{3}$$

where $\omega_i$ denotes the corresponding circular frequency and $\zeta_i$ the corresponding damping ratio.

Separation of Equation (2) into the first $n$ modes and the $N-n$ higher modes yields

$$\ddot{\mathbf{u}}(t) = \sum_{i=1}^{n} \phi_i \Gamma_i \ddot{d}_i(t) + \sum_{i=n+1}^{N} \phi_i \Gamma_i \ddot{d}_i^{(rel)}(t) + \sum_{i=n+1}^{N} \phi_i \Gamma_i \ddot{u}_g(t) \tag{4}$$

In practical applications the evaluation of the response considering all $N$ modes is computationally expensive. In an effort to reduce this expense, the high frequency modal contribution to the relative accelerations, i.e., the second term of the right hand side of Equation (4), is neglected, and the high frequency modal contribution of the ground, i.e., the third term in Equation (4), is expressed in terms of a residual vector, $\mathbf{r}^{(n)}$,

$$\ddot{\mathbf{u}}(t) \approx \sum_{i=1}^{n} \phi_i \Gamma_i \ddot{d}_i(t) + \left( \mathbf{e} - \sum_{i=1}^{n} \phi_i \Gamma_i \right) \ddot{u}_g(t) = \ddot{\mathbf{u}}^{(n)}(t) + \mathbf{r}^{(n)} \ddot{u}_g(t) \ , \quad \mathbf{r}^{(n)} = \mathbf{e} - \sum_{i=1}^{n} \phi_i \Gamma_i \tag{5}$$

This approximation is consistent with the one presented in Pozzi and Der Kiureghian [15, 16]. Since in Equation (3) the term $\omega_i^2 d_i^{(rel)}(t)$ dominates the response for high frequency modes, this proposed approximation of the absolute acceleration response is reasonable [15, 16, 18].

## 3. Ground motion modeling in the frequency domain

The prediction of the seismic structural demand through a response spectrum method is commonly based on an analytical model of the power spectral density (PSD) that characterizes the seismic hazard $\ddot{u}_g$ in the frequency domain. Thus, the influence of the difference between the phase angles is neglected. In the present study the Kanai-Tajimi PSD (subsequently referred to as KT-PSD), defined as [19, 20]

$$G_g^{(KT)}(\nu) = G_0 \frac{1 + 4\zeta_g^2 \left( {}^{\nu}/_{\nu_g} \right)^2}{\left( 1 - \left( {}^{\nu}/_{\nu_g} \right)^2 \right)^2 + 4\zeta_g^2 \left( {}^{\nu}/_{\nu_g} \right)^2} \tag{6}$$

describes the analytical median PSD model. Therein, the normalized PSD of the underlying white noise process, $G_0$, the characteristic frequency of the ground motion, $\nu_g$, and damping ratio, $\zeta_g$, of the ground are calibrated to fit the seismic hazard of the considered site. An excellent overview of different strategies of ground motion modeling in the frequency domain is provided in [21]. For instance, Spanos and Vargas Loli [22] present a statistical approach to design spectrum compatible generation of seismic ground motions, based on an evolutionary power spectrum of a non-stationary stochastic process representing the accelerograms. In this approach the power spectrum of the stochastic seismic ground motion is related to the target spectrum. In a recent development Giaralis and Spanos [23] propose a two-step procedure to generate artificial seismic accelerograms compatible with a given displacement target spectrum. In the first step of this procedure, based on stochastic dynamic analysis a set of simulated non-stationary earthquake records is derived, whose response spectrum is on the average in good agreement with the target spectrum. The agreement depends significantly on the adoption of an appropriate parametric evolutionary power spectral form, related to the target spectrum. In the second step, using the family of harmonic wavelets, simulated records are modify iteratively to satisfy the compatibility criteria for artificial accelerograms proposed in Eurocode 8 [24].

To validate the modal combination rule proposed in this contribution its outcomes are compared with results of RHA. RHA requires a set of ground motions adjusted to the site-specific seismic hazard, which is usually defined in terms of the 5 % damped pseudo-acceleration response spectrum, $S_{ad}$ [2]. In the present study, as an example the seismic hazard representative of Century City (Los Angeles, CA; 34.053 66°N, 118.413 39°W) is considered. In Figure 1 the corresponding response spectrum, $S_{ad}$, is shown by the bold solid line. The spectrum is linearly scaled to the design earthquake spectral response acceleration parameter at short periods (i.e., in the plateau domain of the response spectrum) $S_{DS} = 2.00\,\mathrm{g}$. From the PEER NGA database [25] 92 site compatible ground motion records were selected providing that median and dispersion of the record set matches this design response spectrum and a target dispersion of $\sigma_t = 0.80$ in the frequency range of $0.33\,\mathrm{Hz} \leq {}^{\omega}/_{2\pi} \leq 20\,\mathrm{Hz}$ (i.e., the period range of $0.05\,\mathrm{s} \leq T \leq 3.00\,\mathrm{s}$). The underlying evolutionary record selection algorithm is described in [26]. Figure 1 shows the target design spectrum, the target median $\pm$ one logarithmic standard deviation spectra, individual response spectra of the selected records, and the actual median, 16 % and 84 % quantile spectra.

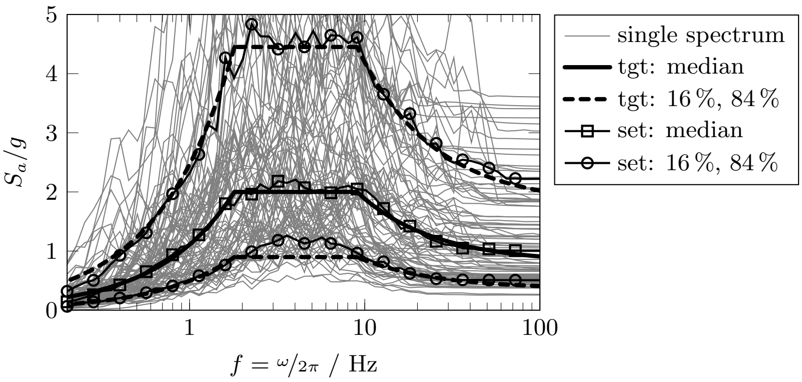


Figure 1: Target response spectra (bold black lines), response spectra of individual records (gray lines), and statistical quantities (lines with markers) for a normal target dispersion $\sigma_t = 0.80$.

The gray line in Figure 2 shows the normalized median of the individual PSDs of the selected ground motion records, $G_g^{(GMs)}$, leaving the integral in the frequency range of $0.01\,\mathrm{Hz} \leq {}^{\nu}/_{2\pi} \leq 20\,\mathrm{Hz}$ to unity,

$$2\pi \int_{0.01}^{20} G_g^{(GMs)}\,\mathrm{d}\nu = \frac{2\pi}{SF} \int_{0.01}^{20} \overline{G}_g^{(GMs)}\,\mathrm{d}\nu = 1 \tag{7}$$

in which $\overline{G}_g^{(GMs)}$ denotes the unscaled median of the individual PSDs of the selected ground motion records. In the present case the scale factor, $SF$, is 1.45. Calibration of the characteristic parameters in the KT-PSD model, Equation (6), to the normalized mean PSD of the records yields $G_0 = 0.18$, ${}^{\nu_g}/_{2\pi} = 1.79\,\mathrm{Hz}$, and $\zeta_g = 0.78$. In Figure 2 the fitted KT-PSD, $G_g^{(KT)}(\nu)$, is shown by a black line. If the damping ratio for the soil model, $\zeta_g$, tends to zero, the peak is located at the central frequency of the PSD. With increasing $\zeta_g$, the peak-frequency of the PSD is shifted to lower frequencies. If $\zeta_g$ tends to infinity, $G_g^{(KT)}(\nu)$ becomes constant. That is, the KT-PSD approaches the underlying white noise process $G_0$, where each frequency is excited by the same power, and thus, higher frequencies contribute more to the response.

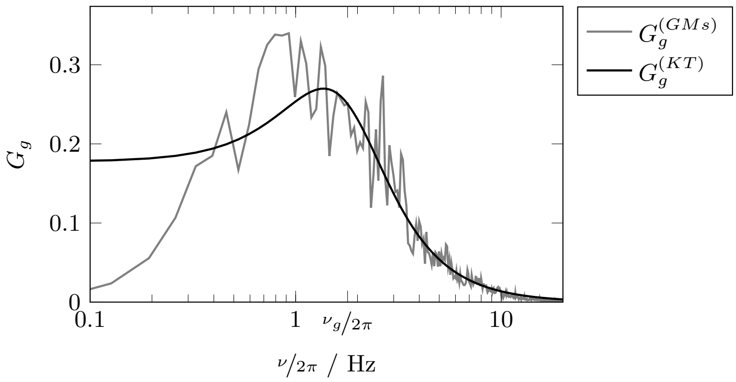


Figure 2: Modeling the ground motion in the frequency domain. Kanai-Tajimi power spectral density (KT-PSD) (black line) fitted to the normalized median PSD of the ground motions (gray line).

## 4. Proposed response spectrum method for total accelerations

Expressing Equation (5) in terms of stationary random vectors [27], i.e., $\ddot{\boldsymbol{U}} \equiv \ddot{\boldsymbol{U}}(t)$, $\ddot{\boldsymbol{U}}^{(n)} \equiv \ddot{\boldsymbol{U}}^{(n)}(t)$, and stationary (modal) random variables, i.e., $\ddot{D}_i \equiv \ddot{D}_i(t)$, $\ddot{U}_g \equiv \ddot{U}_g(t)$, yields

$$\ddot{\boldsymbol{U}} = \sum_{i=1}^{n} \phi_i \Gamma_i \ddot{D}_i + \mathbf{r}^{(n)} \ddot{U}_g = \ddot{\boldsymbol{U}}^{(n)} + \mathbf{r}^{(n)} \ddot{U}_g \tag{8}$$

Assuming that the ensemble of ground motions represents a Gaussian random process with zero mean, $\ddot{U}_g$, the random response vector, $\ddot{\boldsymbol{U}}$, is also Gaussian with zero mean [6]. Consequently, the mean square acceleration, $E\left[\ddot{\boldsymbol{U}}^2\right]$, corresponds to the variance of the response process. This notion allows the definition of the peak value of any arbitrary random variable, here denoted as $X = X(t)$, as the product of the standard deviation, $\sigma_X = \sqrt{Var\,[X]}$, and the peak factor, $p_X$, i.e., $E\left[\max\left(|X|\right)\right] = \sigma_X p_X$ [28]. The peak factor of the response process can be estimated by the mean of the first passage probability [29], as discussed later. Since this concept is used to determine the expected value of the random vector of maximum absolute acceleration demands, $E\left[\max\left(|\ddot{\boldsymbol{U}}|\right)\right]$, the computation of the variance of the response process represented by Equation (8) is required,

$$Var\left[\ddot{\boldsymbol{U}}\right] = Var\left[\ddot{\boldsymbol{U}}^{(n)}\right] + \left(\mathbf{r}^{(n)}\right)^2 Var\left[\ddot{U}_g\right] + 2Cov\left[\ddot{\boldsymbol{U}}^{(n)}, \mathbf{r}^{(n)}\ddot{U}_g\right] \tag{9}$$

The variance of a sum of random variables is equivalent to the double sum of their covariance [30, 31], and thus

$$Var\left[\ddot{\boldsymbol{U}}\right] = \sum_{i=1}^{n}\sum_{j=1}^{n} Cov\left[\ddot{\boldsymbol{U}}_i^{(n)}, \ddot{\boldsymbol{U}}_j^{(n)}\right] + \left(\mathbf{r}^{(n)}\right)^2 Var\left[\ddot{U}_g\right] + 2\sum_{i=1}^{n} Cov\left[\ddot{\boldsymbol{U}}_i^{(n)}, \mathbf{r}^{(n)}\ddot{U}_g\right] \tag{10}$$

Here, $\ddot{\boldsymbol{U}}_i^{(n)}$ denotes the $i$th and $\ddot{\boldsymbol{U}}_j^{(n)}$ the $j$th modal contribution of the multi-modal random vector $\ddot{\boldsymbol{U}}^{(n)}$. The modal vector $\ddot{\boldsymbol{U}}_i^{(n)}$ is expressed in terms of the corresponding mode shape $\phi_i$, effective participation factor $\Gamma_i$, and random modal acceleration $\ddot{D}_i$, yielding

$$\begin{aligned} Var\left[\ddot{\boldsymbol{U}}\right] =& \sum_{i=1}^{n}\sum_{j=1}^{n} \phi_i\Gamma_i\phi_j\Gamma_j Cov\left[\ddot{D}_i, \ddot{D}_j\right] \\ &+ \left(\mathbf{r}^{(n)}\right)^2 Var\left[\ddot{U}_g\right] + 2\mathbf{r}^{(n)}\sum_{i=1}^{n}\phi_i\Gamma_i Cov\left[\ddot{D}_i, \ddot{U}_g\right] \end{aligned} \tag{11}$$

Pearson's cross-correlation coefficient, $\rho_{X,Y}$, of two arbitrary random variables, here denoted as $X$ and $Y$, with zero mean corresponds to their cross-correlation function divided by their root-mean-square (RMS) values. According to the Wiener-Khintchine relations [32, 33], the autocorrelation function and the power spectral density are Fourier transform pairs [6]. Hence, the cross-correlation function and the cross power spectral density of two random processes are Fourier transform pairs too [34, 35]. For strict stationary processes with zero mean the autocorrelation function is constant, and thus, the covariance reduces to the mean square value [6] of a single random variable, i.e., the probability density becomes an universal distribution independent of time [6]. The generalization of this theorem implies that the cross-covariance reduces to the expected value of the product of two random variables each with zero mean. Consequently, their joint probability density is a universal time independent distribution, and thus, the mean of the product of two random variables, $X$ and $Y$, is equivalent to the integral of the cross power spectral density, $G_{XY}(\nu)$. That is, the integral of the mean PSD, which is a statistical average, is a statistical average itself [6], and the correlation coefficient, $\rho_{X,Y}$, reads as

$$\rho_{X,Y} = \frac{Cov\left[X,Y\right]}{\sqrt{Var\left[X\right]Var\left[Y\right]}} = \frac{E\left[XY\right]}{\sqrt{E\left[X^2\right]E\left[Y^2\right]}} = \frac{\displaystyle\int_0^{\infty} G_{XY}(\nu)\,\mathrm{d}\nu}{\sqrt{\displaystyle\int_0^{\infty} G_{XX}(\nu)\,\mathrm{d}\nu \int_0^{\infty} G_{YY}(\nu)\,\mathrm{d}\nu}} \tag{12}$$

Strictly speaking, $\rho_{X,Y}$ represents a *cross-correlation* coefficient since $X$ and $Y$ represent random variables of different processes. However, in this study for simplicity $\rho_{X,Y}$ is just referred to as *correlation coefficient*.

Now, the expected total peak acceleration demand of the $k$th degree of freedom of the structure, $m_{PFA_k}$, can be expressed as the product of the standard deviation and the corresponding peak factor [9],

$$E\left[\max|\ddot{U}_k|\right] \equiv m_{PFA_k} = \sqrt{Var\left[\ddot{U}_k\right]}p_k \tag{13}$$

Note that in a planar frame structure with lumped masses the $k$th degree of freedom corresponds to the $k$th floor. Thus, to put it simple from now on response quantities with subscript $k$ are referred to the $k$th floor.

Accordingly, also the expected $i$th peak modal coordinate is expressed in terms of the corresponding modal peak factor, $p_i$, and the expected peak ground acceleration (PGA) in terms of the peak factor of the ground acceleration, $p_g$,

$$E\left[\max|\ddot{D}_i|\right] \approx S_{a,i} = \sqrt{Var\left[\ddot{D}_i\right]}p_i \tag{14}$$

$$E\left[\max|\ddot{U}_g|\right] \equiv m_{PGA} = \sqrt{Var\left[\ddot{U}_g\right]}p_g \tag{15}$$

in which $S_{a,i}$ denotes the mean pseudo-spectral acceleration at the period of the $i$th mode and $m_{PGA}$ the mean peak ground acceleration. In Equation (14) the total acceleration response spectrum, $E\left[\max|\ddot{D}_i|\right]$, has been approximated by the pseudo-spectral acceleration response spectrum, $S_{a,i}$, providing that the modal damping ratio is small, $\zeta_i \leq 5\,\%$, and the corresponding modal periods are shorter than 7 s [16].

Substituting Equations (12) to (15) into Equation (11) leads to the proposed response spectrum method in terms of the mean PFA demand of the $k$th floor [14],

$$\begin{aligned} E\left[\max\left(|\ddot{U}_k|\right)\right] \equiv m_{PFA_k} = \Bigg[ & \sum_{i=1}^{n}\sum_{j=1}^{n}\frac{p_k}{p_i}\frac{p_k}{p_j}\Phi_{i,k}\Gamma_i S_{a,i}\Phi_{j,k}\Gamma_j S_{a,j}\rho_{i,j} \\ & + \left(\frac{p_k}{p_g}m_{PGA}r_k^{(n)}\right)^2 + 2m_{PGA}\,r_k^{(n)}\frac{p_k}{p_g}\sum_{i=1}^{n}\frac{p_k}{p_i}\Phi_{i,k}\Gamma_i S_{a,i}\rho_{i,g}\Bigg]^{\frac{1}{2}} \end{aligned} \tag{16}$$

Herein, $r_k^{(n)}$ is the $k$th element of $\mathbf{r}^{(n)}$ (Equation (5)), and $\phi_{i,k}$ the $k$th element of $\phi_j$. Note that at this stage the correlation coefficient between the $i$th and $j$th modal total acceleration, $\rho_{i,j}$, the correlation coefficient between the $i$th modal total acceleration and the ground, $\rho_{i,g}$, and the peak factors $p_k$, $p_i$ and $p_g$, are unknown.

Response quantities due to earthquake excitation are assumed to be lognormal distributed [36, 37]. Consequently, in the ground motion selection procedure the central value of the record set is represented by the median rather than the mean, see Figures 1 and 2. Hence, in Equation (16) the mean, $m_{PFA_k}$, must be substituted by the median, $\breve{m}_{PFA_k}$. Accordingly, the same substitution must be applied to mean peak factors and mean pseudo-acceleration spectral ordinates. In the subsequent considerations in all equations the median instead of the mean is employed without changing the designations of the affected variables.

## 5. Cross-spectral moments, correlation coefficients, and peak factors

### 5.1. Definition of cross-spectral moments

For further derivations the $l$th cross-spectral moment, $\lambda_{l,XY}$, of two arbitrary random response variables, $X$ and $Y$ is defined [9],

$$\lambda_{l,XY} = \int_0^\infty \nu^l G_{XY}(\nu)\,\mathrm{d}\nu = \int_0^\infty \nu^l G_g^{(KT)}(\nu) H_X(\nu) H_Y^*(\nu)\,\mathrm{d}\nu \quad , \quad l = 0, 1, 2, ... \tag{17}$$

based on the description of the ground excitation by the KT-PSD, $G_g^{(KT)}(\nu)$, Equation (6). $H_X(\nu)$ and $H_Y(\nu)$ are transfer functions (often referred to as frequency response functions (FRFs)), the asterisk denotes the complex conjugate. The *spectral moment*, $\lambda_{l,XX}$, is the cross-spectral moment for one random variable, $X$. As it is subsequently shown, the analysis of the correlation coefficients in Equation (16) is based on the zeroth ($l = 0$) spectral and cross-spectral moments, for the peak factors additionally the first and the second ($l = 1, 2$) spectral and cross-spectral moments are required.

### 5.2. Relation between cross-spectral moments and correlation coefficients

Comparison of Equation (17) with Equation (12) reveals that the correlation coefficients present in Equation (16) can be expressed by means of the corresponding zeroth cross-spectral moment ($l = 0$),

$$\rho_{i,j} = \frac{\lambda_{0,ij}}{\sqrt{\lambda_{0,ii}\lambda_{0,jj}}} \qquad \rho_{i,g} = \frac{\lambda_{0,ig}}{\sqrt{\lambda_{0,ii}\lambda_{0,gg}}} \tag{18}$$

Inserting the FRF of the $i$th total modal acceleration,

$$H_i(\nu) = \frac{\omega_i^2 + 2\mathbb{i}\zeta_i\omega_i\nu}{\omega_i^2 - \nu^2 + 2\mathbb{i}\zeta_i\omega_i\nu} \tag{19}$$

and its $j$th modal counterpart into Equation (17) yields the cross-spectral moment $\lambda_{0,ij}$. Spectral moments $\lambda_{0,ii}$ and $\lambda_{0,jj}$ are obtained by substituting two times $H_i(\nu)$, respectively $H_j(\nu)$ into Equation (17). When evaluating $\lambda_{0,ig}$ and $\lambda_{0,gg}$, $H_g(\nu) = 1$ is inserted because for a rigid modal SDOF oscillator (as it is the ground), the natural circular frequency is infinity, and consequently, the FRF $H_g(\nu)$ is unity.

### 5.3. Peak factors and the first-passage probability

The zeroth spectral moments (i.e., $i = j$) can be interpreted as mean-square total acceleration, i.e., $\lambda_{0,ii} = Var\left[\ddot{D}_i\right]$. Consequently, the $i$th modal peak factor, $p_i$, corresponds to the ratio of the pseudo-spectral acceleration (known through the response spectrum, $S_{a,i}$) at natural frequency $\omega_i$ to the root of the zeroth spectral moment, $\sqrt{\lambda_{0,ii}}$, compare with Equation (14).

Accordingly, the peak factor of the ground, $p_g$, corresponds to the ratio of the known pseudo-spectral acceleration at infinite frequency to the root of the zeroth spectral moment, $\sqrt{\lambda_{0,gg}}$, see Equation (15).

The peak factor of the response process for the $k$th floor, $p_k$, is the only remaining parameter of Equation (16) to be evaluated. As discussed in several studies such as [38, 39, 29], an estimation of any response quantity of a normal stationary process can be computed if the first-passage probability is available. Since the objective of this study is to provide a simple modal combination rule with an analytical foundation, the computation of peak factor $p_k$ is based on the common assumption of the first-passage probability for normal stationary random processes $X(t)$ with zero mean as proposed by Vanmarcke [29],

$$F_R\left(r\right) = P\left[R \leq r\right] = \left(1 - \exp\left(-\frac{r^2}{2}\right)\right) \exp\left(\frac{-2 f_a t \left(1 - \exp\left(-\sqrt{\frac{\pi}{2}} q_e r\right)\right)}{1 - \exp\left(-\frac{r^2}{2}\right)}\right) \tag{20}$$

instead of the first-passage probability of a *non-stationary* random process, which would be a more realistic representation of an ensemble of ground motions [40]. The reduced barrier level [29],

$$r = \frac{edp}{\sigma_X} = \frac{edp}{\sqrt{\lambda_0}} \tag{21}$$

is the numerical value (the barrier or a threshold level) that separates the *safe* and the *unsafe* response values of the *engineering demand parameter* (EDP; here the demand $PFA_k$) of interest [39, 29] normalized with respect to the RMS value, $\sigma_X$, of the underlying random process $X(t)$. The mean rate of B-crossings [41], defined as crossings of the barrier level from below [39, 29], is

$$f_a = f_0 \exp\left(-r^2/2\right) = \frac{1}{2\pi}\sqrt{\frac{\lambda_2}{\lambda_0}} \exp\left(-r^2/2\right) \tag{22}$$

where $f_0$ denotes the zero up-crossing rate [29], often referred to as the average frequency of the response process [38]. Consequently, the average period of the response process is

$$T_0 = \frac{1}{f_0} = \frac{2\pi}{\sqrt{\frac{\lambda_2}{\lambda_0}}} \tag{23}$$

The shape factor of the PSD [42] of the response process reads as

$$q = \sqrt{1 - \frac{\lambda_1^2}{\lambda_0 \lambda_2}} \tag{24}$$

According to [29] the empirical shape factor, $q_e$, is an empirical modification of $q$ by the power of a constant $b = 1.20$,

$$q_e = q^b \tag{25}$$

The evaluation of Equations (21) to (24) requires the first three spectral moments of the response process, i.e., $\lambda_0, \lambda_1$ and $\lambda_2$. While Vanmarcke [42] and Der Kiureghian [9] already have discussed the derivation of spectral moments and their physical and geometric interpretation for displacements relative to the base in detail, the properties of cross-spectral moments for the total acceleration response are explained in the subsequent subsection.

Ideally, the probabilistic distribution of $R$ would be identical to the distribution obtained from RHA. However, the traditional assumption in earthquake engineering of a log-normally distributed seismic response behavior [43, 36] is inconsistent with the CDF of the first passage probability in Equation (20). Preliminary studies of the authors have revealed that the difference between the log-normal CDF and the first passage probability is small in domains close the central value. Additionally the log-normal distribution is fully determined by the mean and dispersion of the corresponding normal distribution ($m$ and $\sigma$) [31]. For a first step towards the PFA assessment with the proposed closed form solution, the remainder of this paper focuses on the estimation of the median results only rather than the approximation of the complete statistical distribution, or approximation of the dispersion according to a log-normal distribution as assumed for response quantities in earthquake engineering. Thus, the strategy in this paper is to estimate the median of log-normal distributed PFA demands by the mean of the first passage probability of the corresponding response process. Generally, the expected value of a positive monotonic increasing function of an arbitrary random variable $X$ can be determined if the CDF of the random variable is available. Rewriting the expected value in terms of a *Riemann-Stieltjes* integral [44] and subsequent application of integration by parts yields

$$E\left[g(X)\right] = \int_0^\infty g(x)\,\mathrm{d}F_X(x) = \int_0^\infty \frac{\mathrm{d}g}{\mathrm{d}x}\left(1 - F_X(x)\right)\mathrm{d}x \tag{26}$$

which is also referred to as the *law of the unconscious statistician*. Evaluating this integral for the first passage probability according to Equation (20) reads

$$m_R = E[R] = \int_0^\infty \left(1 - F_R(r)\right)\mathrm{d}r \tag{27}$$

in which an adequate approximation of the first passage time, $t$, is the average period of the response process, $T_0$, see Equation (23).

Specialization of the *edp* in Equation (21) for the expected value of the PFA demand in the $k$th floor,

$$m_{R_k} = \frac{m_{PFA_k}}{\sigma_{\ddot{U}_k}} \tag{28}$$

and comparison with Equations (13) to (15), respectively, reveals that $m_{R_k}$ corresponds to the desired peak factor $p_k$ of the median PFA demand in the $k$th floor.

Based on these foundations the analysis of the peak factors for the proposed modal combination rule can be summarized as follows. Since evaluation of Equations (22) to (24) requires the appropriate zeroth, first and second multi-modal spectral moments, in a first step these quantities are determined. The spectral moments of the response process, $\ddot{U}_k$, are determined as follows. The covariance reduces to the autocorrelation function for a zero mean process, and thus, the concept of uni-modal spectral moments can be applied to the multi-modal spectral moments of the response process [8]. Consequently, Equation (11) represents the zeroth spectral moment of the response process, which can be rewritten in terms of the expansion of modal cross-spectral moments [8]. For the $k$th floor the $l$th multi-modal spectral moment reads

$$\lambda_{l,k} = \sum_{i=1}^{n}\sum_{j=1}^{n} \phi_{i,k}\Gamma_i\phi_{j,k}\Gamma_j\lambda_{l,ij} + \left(r_k^{(n)}\right)^2 \lambda_{l,gg} + 2r_k^{(n)}\sum_{i=1}^{n}\phi_{i,k}\Gamma_i\lambda_{l,ig} \tag{29}$$

As it will be shown later, the first and second moments of the ground acceleration, $\lambda_{1,gg}$ and $\lambda_{2,gg}$, appearing in the last term are infinite. Thus, in Equation (29) the second and third term associated to spectral moments of the ground are neglected, leading to the following approximation

$$\lambda_{l,k} \approx \sum_{i=1}^{n}\sum_{j=1}^{n} \phi_{i,k}\Gamma_i\phi_{j,k}\Gamma_j\lambda_{l,ij}, \quad l = 0, 1, 2 \tag{30}$$

The physical interpretation of Equation (30) is equivalent to disregarding truncated modes, which is physically more meaningful than simply neglecting the infinite terms.

With the now readily available spectral moments, Equations (22) to (25), and Equation (20), are analyzed. Substituting the outcome of Equation (20) into Equation (27) its evaluation finally results in the desired peak factor, $p_k$.

*5.4. Analytical cross-spectral moments for modal total accelerations*

Substituting Equation (19) into Equation (17) yields the actual integrals for the cross-spectral moments to be evaluated. Cauchy's residue theorem is applied to solve the integrals for the zeroth and second cross-spectral moment ($l = 0, 2$), yielding

$$\lambda_{0,ij} = G_0 \pi \omega_i \omega_j \nu_g \left[ \frac{\sum\limits_{m=0}^{2} \sum\limits_{n=0}^{2} \zeta_i^m \zeta_j^n \xi_{0,mn}(\omega_i, \omega_j)}{4\zeta_g D_4} + \frac{2\nu_g \sum\limits_{m=0}^{4} \sum\limits_{n=0}^{2} \zeta_i^m \zeta_j^n \psi_{0,mn}(\omega_i, \omega_j)}{D_1} \right] \tag{31}$$

$$\lambda_{2,ij} = G_0 \pi \omega_i \omega_j \nu_g^2 \left[ \frac{\nu_g \sum\limits_{m=0}^{2} \sum\limits_{n=0}^{2} \zeta_i^m \zeta_j^n \xi_{2,mn}(\omega_i, \omega_j)}{4\zeta_g D_4} + \frac{2\omega_i^2 \sum\limits_{m=0}^{6} \sum\limits_{n=0}^{2} \zeta_i^m \zeta_j^n \psi_{2,mn}(\omega_i, \omega_j)}{D_1} \right] \tag{32}$$

Evaluation of the first cross-spectral moment requires a partial fraction decomposition because the integrand is antisymmetric (consequently, integration by Cauchy's residue theorem for the integration limits from minus to plus infinity yields zero). The result reads

$$\begin{aligned}
\lambda_{1,ij} = G_0 \omega_i \omega_j \nu_g^2 \Bigg[ & \omega_i \left( \frac{\pi}{2} - \arctan\left( \frac{\zeta_i}{\sqrt{1-\zeta_i^2}} \right) \right) \left( \frac{\sum\limits_{m=0}^{6} \sum\limits_{n=0}^{2} \zeta_i^m \zeta_j^n \psi_{1,mn}(\omega_i, \omega_j)}{\sqrt{1-\zeta_i^2} D_1} \right) \\
& + \omega_j \left( \frac{\pi}{2} - \arctan\left( \frac{\zeta_j}{\sqrt{1-\zeta_j^2}} \right) \right) \left( \frac{\sum\limits_{m=0}^{6} \sum\limits_{n=0}^{2} \zeta_i^n \zeta_j^m \psi_{1,mn}(\omega_j, \omega_i)}{\sqrt{1-\zeta_j^2} D_2} \right) \\
& + \left( \arctan\left( \frac{\zeta_g}{\sqrt{1-\zeta_g^2}} \right) - \frac{\pi}{2} \right) \left( \frac{\sum\limits_{m=0}^{2} \sum\limits_{n=0}^{2} D_4 \zeta_i^m \zeta_j^n \xi_{1,mn}(\omega_i, \omega_j) + D_3 \zeta_i^n \zeta_j^m \xi_{1,mn}(\omega_j, \omega_i)}{4\zeta_g \sqrt{1-\zeta_g^2} D_3 D_4} \right) \\
& + \omega_i \ln(\omega_i) \left( \frac{\sum\limits_{m=0}^{5} \sum\limits_{n=0}^{2} \zeta_i^m \zeta_j^n \hat{\psi}_{1,mn}(\omega_i, \omega_j)}{D_1} \right) + \omega_j \ln(\omega_j) \left( \frac{\sum\limits_{m=0}^{5} \sum\limits_{n=0}^{2} \zeta_i^n \zeta_j^m \hat{\psi}_{1,mn}(\omega_j, \omega_i)}{D_2} \right) \\
& + \ln(\nu_g) \left( \frac{\sum\limits_{m=0}^{2} \sum\limits_{n=0}^{2} D_3 \zeta_i^m \zeta_j^n \hat{\xi}_{1,mn}(\omega_i, \omega_j) + D_4 \zeta_i^n \zeta_j^m \hat{\xi}_{1,mn}(\omega_j, \omega_i)}{2\zeta_g D_3 D_4} \right) \Bigg]
\end{aligned} \tag{33}$$

Functionals $\xi_{l,mn}(\omega_i, \omega_j), \psi_{l,mn}(\omega_i, \omega_j)$, etc., in the summands of these equations are sorted with respect to the exponent of the damping ratios, $m$ and $n$, which allows us to linearize the CQC combination rule with respect to the damping coefficients. In the Appendix the resulting cross-spectral moments including all required functions and functionals are listed. The subscript $l$, $l = 0, 1, 2$, of $\xi_{l,mn}$ denotes the functional for the $l$th cross-spectral moment. This notation allows the definition of matrices of functionals, $\mathbf{\Xi}_l$ and $\mathbf{\Psi}_l$, as shown in detail in the Appendix. The column and row indexes, $m$ and $n$, of these matrices start at zero to be consistent with the exponent of the damping ratios.

The $l$th cross-spectral moment between the $i$th modal acceleration and the ground acceleration, $\lambda_{l,ig}$, is derived from $\lambda_{l,ij}$ setting the limit of $\omega_j$ to infinity,

$$\lim_{w_j \to \infty} \left(\lambda_{l,ij}\right) = \lambda_{l,ig} \tag{34}$$

### *5.5. Behavior of the correlation coefficients*

Substitution of the zeroth cross-spectral moments, defined in Equation (31), into Equation (18) yields the correlation coefficients. Figure 3 shows the correlation coefficients between the modal total accelerations, $\rho_{i,j}$, in the frequency domain for damping ratios $\zeta_i = \zeta_j = 0.05$. It is readily observed that for closely spaced modes correlation is important. For instance, from Figure 3b it can be observed that an offset from the diagonal along the normalized $\omega_i$ or $\omega_j$ axis of about 1 Hz reduces the correlation coefficient only to $\rho_{i,j} = 0.75$. For high frequency modes, i.e., ${}^{\omega_i}/_{2\pi} \gg 5\,\mathrm{Hz}$ and ${}^{\omega_j}/_{2\pi} \gg 5\,\mathrm{Hz}$, the minimum correlation coefficient is approximately $\rho_{i,j} = 0.25$.

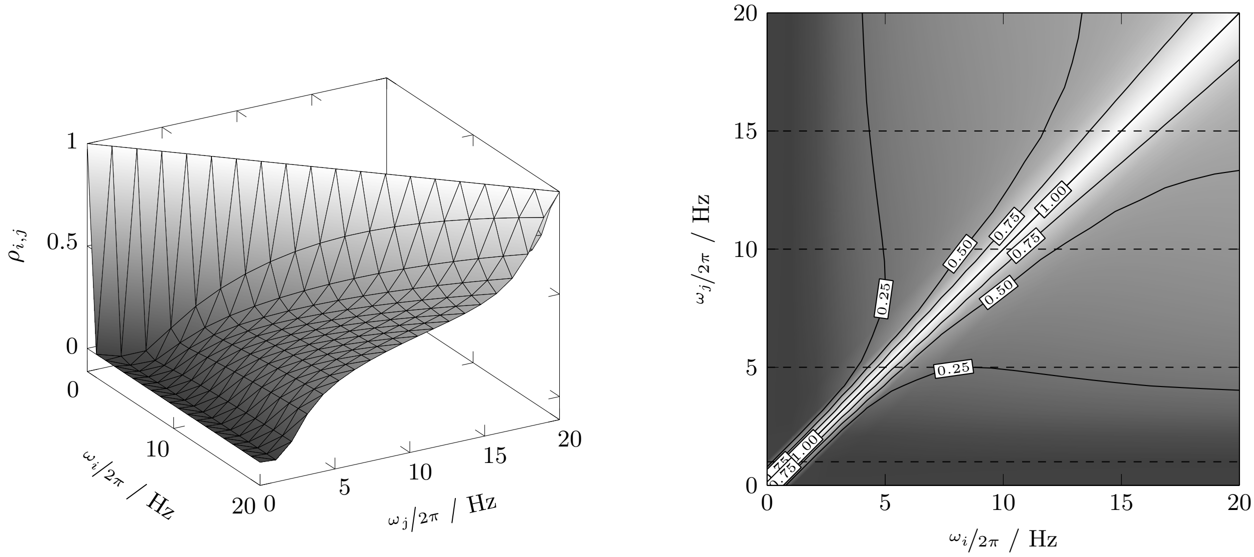


(a)

(b)

Figure 3: Modal correlation coefficient, $\rho_{i,j}$, for $\zeta_i = \zeta_j = 0.05$. (a) Surface plot, and (b) contour plot.

Figure 4a shows the correlation coefficients based on damping ratios $\zeta = \zeta_i = \zeta_j = 0.01$, 0.05 and 0.10, respectively, for frequencies ${}^{\omega_j}/_{2\pi} = 1\,\mathrm{Hz}$, 5 Hz, 10 Hz and 15 Hz. In Figure 3b these frequencies are highlighted by dashed lines. These figures confirm that the correlation between the modes increases with growing damping, leading to a wider distribution of the correlation coefficient around full correlation for $\omega_i = \omega_j$. It is evident that the correlation is dominant in the domains of resonance. However, if $\omega_i$ exceeds the resonance frequency $\omega_j$, $\omega_i \gg \omega_j$, the correlation in these frequency regions is also considerably large, and the correlation coefficient ranges approximately between $\rho_{i,j} \approx 0.20$ for $\zeta_i = \zeta_j = 0.01$, and $\rho_{i,j} \approx 0.75$ for $\zeta_i = \zeta_j = 0.10$. Consequently, this frequency domain is characterized by a relatively strong correlation regardless of the modal separation. Comparable results where obtained by Pozzi and Der Kiureghian [15, 16] and Taghavi and Miranda [13, 14] for total acceleration demands based on numerical evaluations, and by Der Kiureghian and Nakamura [18] for modal displacement demands in the high frequency domain.

Figure 4b shows the correlation coefficient between the modal total acceleration and the ground acceleration, $\rho_{i,g}$, Equation (18), as a function of normalized frequency ${}^{\omega_i}/_{2\pi}$. It is revealed that the correlation coefficient strongly depends on the damping ratio. For high frequency modes, $\omega_i \gg \nu_g$, $\rho_{i,g}$ approaches unity, indicating a quasi-static response [18] of this particular mode. This becomes obvious from evaluation of Equation (3), because if $\omega_i$ approaches infinity, the largest contribution to balance the right side of this equation is associated to the third term, $\omega_i^2 d_i^{(rel)}(t)$. Consequently, the first and second term can be neglected, and the response becomes quasi-static. If the damping ratio increases, the second term of Equation (3) significantly contributes to the response, graphically shown in Figure 4b. This results are consistent with observations of Pozzi and Kiureghian [15], and Taghavi and Miranda [13, 14].

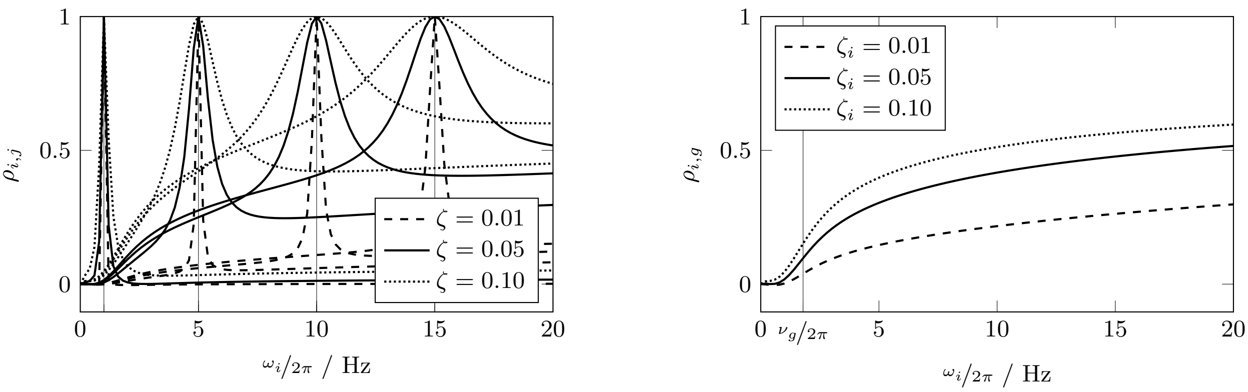


(a) (b)

Figure 4: (a) Influence of different damping ratios, $\zeta = \zeta_i = \zeta_j = 0.01$, 0.05 and 0.10, on modal correlation coefficient $\rho_{i,j}$, and (b) correlation coefficient $\rho_{i,g}$ for the $i$th modal total acceleration and the ground acceleration.

## 6. Application

### 6.1. Planar structures

In a first series of application the proposed CQC method is employed to estimate the PFA demands of a six-, a twelve-, and a 24-story generic elastic, planar, regular single-bay steel moment resisting frame (referred to as SMRF) subjected to the Century City record set. These frame structures exhibit the following properties.

- Fundamental modal properties: The fundamental period is determined by the simplified procedure according to ASCE 7-10 [2], and depends on the number of stories and the type of the load bearing structure. The fundamental mode shape is assumed to be linear.
- Seismic mass: The seismic active mass per floor, $2 \times m_f = 2 \times 45.36 \times 10^3$ kg, is concentrated in the beam-column (BC) connections. To each BC connection the same mass is applied, except at the roof level, where only the half is used. This mass distribution leads to more realistic responses since the structure is designed for lateral loads only.
- Geometric properties: For all structures, the story height is $h = 3.66$ m, and the bay width is assumed to be $b = 2h$.
- Stiffness: Young's modulus for steel is assumed to be $E_S = 2.10 \times 10^{11}\,\mathrm{N/m^2}$.
- Damping: Rayleigh type damping is considered with a modal damping ratio of $\zeta = 0.05$ assigned to the frequency of the first mode and to the frequency of the 95 % cumulative mass participating mode.

Detailed information regarding the computation of structural and modal properties can be found in [45]. The remaining structural properties are determined by the procedure described in Medina and Krawinkler [46].

The application of the proposed response spectrum method is described in detail for the six-story SMRF structure. The amplitudes of the mode shapes at the story levels expressed in terms of the normalized height of the structure, $h_{rel}$, and the modal properties of the six-story frame are listed in Tables 1 and 2. In Table 2 $T_i = 2\pi/\omega_i$ denotes the $i$th structural period. It is important to note that for a correct estimation of the peak factors the median PSD and the median response spectrum must be consistent. Thus, it is essential to substitute the scaled average PSD, $\overline{G}_g^{(GMs)}$ (the integrand in Equation (7)), into the corresponding equations.

Table 1: Mode shapes of the six-story SMRF structure.

| $h_{rel}$ | mode shapes | | | | | |
|---|---|---|---|---|---|---|
| | $\phi_1$ | $\phi_2$ | $\phi_3$ | $\phi_4$ | $\phi_5$ | $\phi_6$ |
| 1/6 | 0.17 | −0.26 | −0.50 | −0.91 | −0.95 | 0.75 |
| 2/6 | 0.33 | −0.44 | −0.64 | −0.54 | 0.31 | −1.00 |
| 3/6 | 0.50 | −0.48 | −0.25 | 0.70 | 0.85 | 0.74 |
| 4/6 | 0.67 | −0.30 | 0.46 | 0.82 | −1.00 | −0.35 |
| 5/6 | 0.83 | 0.15 | 0.74 | −1.00 | 0.44 | 0.09 |
| 6/6 | 1.00 | 1.00 | −1.00 | 0.54 | −0.14 | −0.02 |

Table 2: Modal properties of the six-story SMRF structure.

| $i$ | $\Gamma_i$ | $T_i$ / s | $\omega_i$ / rad/s | $\zeta_i$ |
|---|---|---|---|---|
| 1 | 1.48 | 0.86 | 7.33 | 0.05 |
| 2 | −0.74 | 0.34 | 18.44 | 0.04 |
| 3 | −0.35 | 0.20 | 30.74 | 0.05 |
| 4 | −0.19 | 0.13 | 48.20 | 0.07 |
| 5 | −0.14 | 0.09 | 73.48 | 0.10 |
| 6 | 0.10 | 0.06 | 106.63 | 0.14 |

Figure 5a shows the PFA demands of each story of the six-story structure, subsequently referred to as profiles. To evaluate the accuracy of these outcomes additionally the “exact” reference results of RHA are depicted: the PFA profiles for each single record of the complete set are shown by gray thin lines, and the corresponding median by a solid thick black line. For the sake of completeness the corresponding 16 % and 84 % quantiles are also depicted. Solid lines with markers refer to the median PFA demands obtained from modal combination rules. Circular markers refer to the outcome of the proposed CQC rule based on a first mode approximation, diamond markers refer to the CQC solution when considering the 95 % cumulative mass participating modes. Additionally, triangular markers highlight the first mode approximation using the common SRSS method [5]. It is seen that for this particular structure subjected to the Century City record set the first mode representation of the proposed CQC method yields a reasonable approximation of the median PFA demands, in contrast to the first mode approximation of the traditional SRSS method. Since the first mode is linear, the spatial redistribution of the first mode pseudo spectral acceleration based on the SRSS rule is linear too. The first mode PFA approximation of the CQC rule is, however, nonlinear because the residual vector $\mathbf{r}_n$ contains truncated modes, which describe the spatial distribution of the PGA, included in the second and the third term of Equation (16). The peak factors modify the amplitudes of the first mode PFA approximation but do not impose additional nonlinearities to the PFA profile, because the median peak factor of the response process, $p_k$, is almost constant with respect to the story number, as it is shown in Figure 5b, and the fundamental modal peak factor is obviously not affected by the story number. When including the 95 % cumulative mass participating modes in the proposed CQC modal combination rule, its outcome matches the “exact” median PFA profiles based on RHA very well.

Figure 5b shows profiles of the peak factors $p_k$ at the $k$th floor level, $k = 0, ..., 6$, for different number of modes approximating the median PFA demand. At the base ($k = 0$), i.e., at $h_{rel} = 0$, the depicted peak factor corresponds to the peak factor of ground acceleration, $p_g$. It is seen that the variation of $p_k$ from the first to the sixth floor is small. Considering the fundamental mode only, $p_k$ is the same for all floors, under-predicting at each floor the $p_k$ profile including all modes. In contrast, a three mode approximation of $p_k$ is close to its full mode description.

Figure 6 shows the median PFA profiles of a twelve-story ($\omega_1 = 4.22$ rad/s) and a 24-story ($\omega_1 = 2.42$ rad/s) SMRF structure. A full description of the modal properties of these structures can be found in [45]. Thin lines with markers represent median PFA demand approximations found by the proposed CQC response spectrum method based on different numbers of modes: circular markers correspond to a fundamental single mode approximation, square markers to a two mode approximation, and triangle markers to the outcome considering all modes up to the 95 % cumulative mass participating mode. The “exact” median PFA demand obtained from RHA is shown by a bold solid line. For both structures the single mode CQC approximation of the median PFA demand is nonlinear with respect to the structural height because the last two terms of Equation (16) contain truncated modes, as discussed before. When including two modes, the results of the proposed CQC rule follow the shape of “exact” PFA profiles. However, in

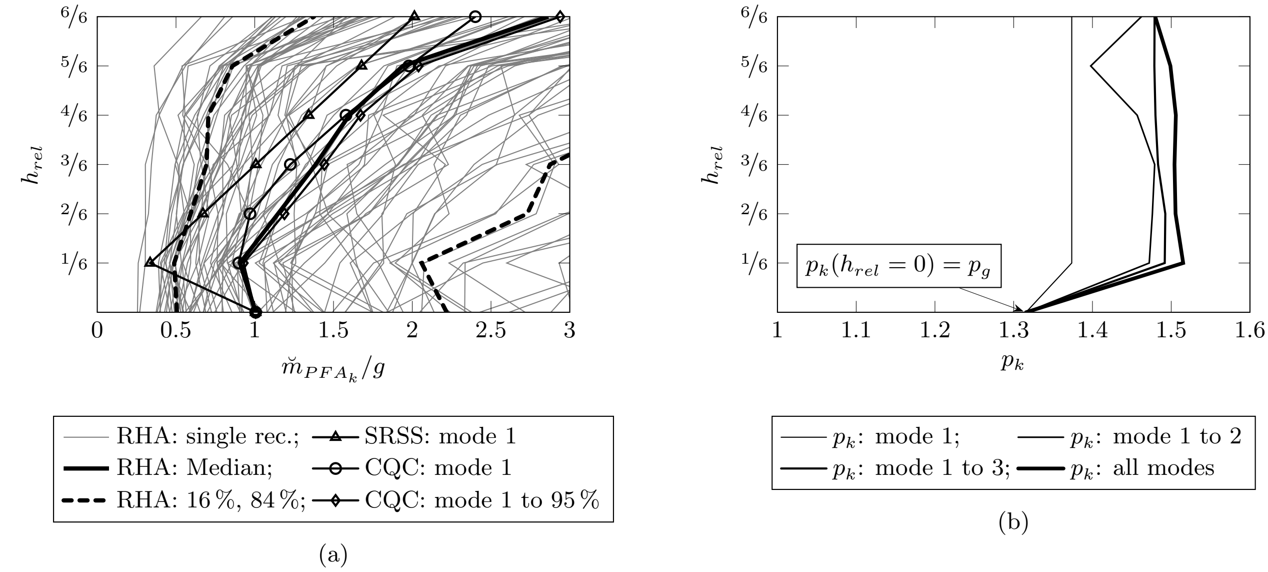


Figure 5: (a) PFA demand profiles of a six-story SMRF structure. RHA benchmark solution (median and quantiles), median PFA outcomes of the CQC modal combination rule based on a single mode, and 95 % cumulative mass participating modes, respectively, and single mode SRSS method approximation. (b) Corresponding median peak factor profiles considering different number of modes.

particular for the 24-story structure the roof PFA demand is under-predicted by almost a factor of two, whereas considering the 95 % cumulative mass participating modes yields to close match of the roof PFA demand.

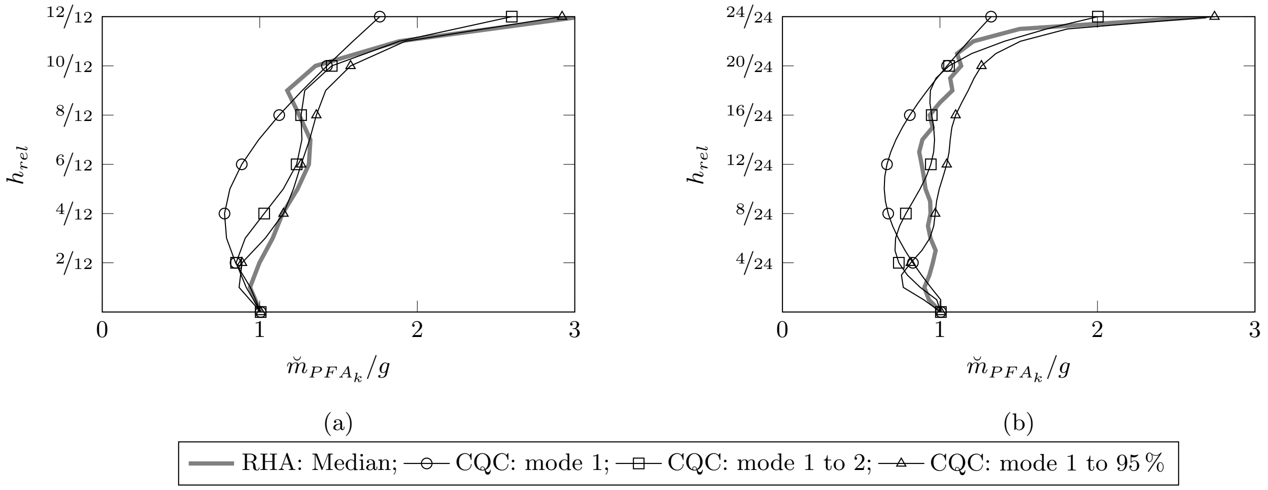


Figure 6: Median PFA demand profiles of (a) a twelve-story SMRF structure, and (b) a 24-story SMRF structure. RHA benchmark solution and outcomes of the CQC modal combination rule based on one mode, two modes, and 95 % cumulative mass participating modes, respectively.

*6.2. Spatial structures*

For further evaluation of the proposed CQC rule spatial six-story, twelve-story, and 24-story generic structures are analyzed, which represent an extension of the previously considered planar frames to the spatial domain. Each floor of these structural models is composed of four massless columns and a horizontal rigid diaphragm, to which an eccentric lumped mass is assigned. The lumped mass at the roof level is only half of the lumped mass at the story levels within the building. Two types of structures are considered: SMRF structures, and structures composed of shear walls (referred to as WALL). Each column of an SMRF structure is modeled as a simple beam-column element with discrete elastic springs at both ends, representing the flexural stiffness of the story beams. The models of the WALL structures are composed of the same elements, however, they are stiffer in the lateral direction than SMRFs. Consequently, the modal properties of SMRF and WALL generic structures are also different: the fundamental mode shape of a symmetric SMRF structure (i.e., the lumped masses are centered) is assumed to be linear, while for a symmetric WALL structure a parabolic shape with respect to the height is assumed. In the considered generic spatial structures the center of mass of each rigid floor is eccentric with respect to the center of stiffness: $\mathbf{e}_M = [x = 0.30\,\mathrm{m}, y = 0.30\,\mathrm{m}]^\intercal$ (schematically depicted in Figure 7a). Thus, these structures exhibit closely spaced modes, which is desirable for evaluation of the proposed CQC modal combination rule. Figure 7b shows a sketch of the lower stories of these structures. The fundamental frequencies of the structures match the values given in ASCE 7-10 [2]. The first three angular natural frequencies are: $\omega_1 = 7.20\,\mathrm{rad/s}$, $\omega_2 = 7.33\,\mathrm{rad/s}$, $\omega_3 = 7.96\,\mathrm{rad/s}$ (six-story SMRF); $\omega_1 = 4.14\,\mathrm{rad/s}$, $\omega_2 = 4.21\,\mathrm{rad/s}$, $\omega_3 = 4.59\,\mathrm{rad/s}$ (twelve-story SMRF); $\omega_1 = 2.38\,\mathrm{rad/s}$, $\omega_2 = 2.42\,\mathrm{rad/s}$, $\omega_3 = 2.64\,\mathrm{rad/s}$ (24-story SMRF); $\omega_1 = 12.58\,\mathrm{rad/s}$, $\omega_2 = 12.59\,\mathrm{rad/s}$, $\omega_3 = 31.48\,\mathrm{rad/s}$ (six-story WALL); $\omega_1 = 7.55\,\mathrm{rad/s}$, $\omega_2 = 7.55\,\mathrm{rad/s}$, $\omega_3 = 30.95\,\mathrm{rad/s}$ (twelve-story WALL); $\omega_1 = 4.49\,\mathrm{rad/s}$, $\omega_2 = 4.49\,\mathrm{rad/s}$, $\omega_3 = 28.2\,\mathrm{rad/s}$ (24-story WALL). Rayleigh type damping is considered with a modal damping ratio of $\zeta = 0.05$ assigned to the fundamental mode and to the 95 % cumulative mass participating mode. Further details to these structures are found in [45].

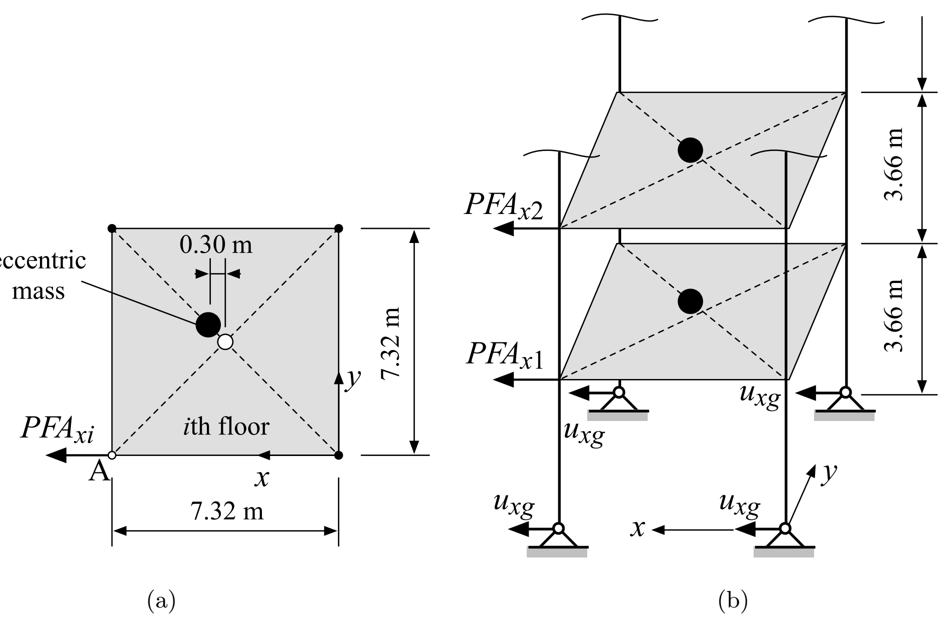


Figure 7: (a) Plane view of the eccentric mass at the $k$th floor level, and (b) isometric view of the first two stories of the spatial structure.

To provide the "exact" PFA demands, RHA is conducted exposing the structures in the $x$-direction to the 92 ground motions of the Century City record set. That is, each support is excited by the same ground acceleration series, which represents the second derivative of the ground displacement $u_{xg}$. For each ground motion the PFA demand is computed at each floor level for corner point $A$ in the $x$-direction, $PFA_k, k = 1, 2, ..., N$, see Figure 7, and subsequently, the median demand is determined.

In Figure 8 the "exact" median profiles obtained from RHA are depicted by a thick solid line. The results of the left column refer to the six-story (first row), the twelve-story (second row), and the 24-story (third row) SMRF structure, those of the right column to the WALL structures in the same sequence. As observed, the median PFA demand of the WALL buildings is larger compared to the outcomes of the SMRF structures. This can be explained by the fact that the first few periods of the the WALL structures are close to the corner periods of the median response spectrum, and thus, contribute significantly to the PFA response. Moreover, with increasing height of the WALL structures the S-shape of the median PFA demand becomes dominant, and consequently, simplified estimation of this response quantity by a straight line, such as proposed in [2], is deemed to fail.

The response approximations obtained by the proposed CQC method considering different number of modes are also shown in the same figure. It is seen that this method yields excellent predictions of the median PFA demand of the low- (six-story) and mid-rise (twelve-story) spatial buildings when considering 95% modal mass participation modes, represented by the graphs with triangle markers (Figures 8a to 8d). Approximations of profiles on the high-rise 24-story buildings are still adequate. For instance, the median PFA demand of the SMRF structure between the base and 20 % of the relative height is slightly underestimated by the CQC method, see Figure 8e. In contrast, the proposed method leads to moderate PFA overestimations, see Figure 8f. These differences can be led back to the assumptions of the normal stationary random vibration theory, in which stationary Gaussian random processes represent a rough approximation of recorded ground motions.

Comparison of PFA approximations by the proposed CQC method (Figure 8) and by the common SRSS rule [5] (Figure 9) demonstrates the superiority of the novel approach. The common SRSS method neither accounts for modal correlation, nor considers peak factors and truncated modes. Thus, the graphs with circular markers in Figure 9 are indeed proportional to the fundamental mode only, i.e., an almost linear variation with respect to height for SMRF structures and an almost parabolic variation for WALL structures. As previously discussed, the fundamental mode approximation of the PFA demand based on the proposed CQC method (see Figure 8) is nonlinear because truncated modes are included, thus improving the median PFA demand prediction at the lower floor levels compared to the common SRSS rule.

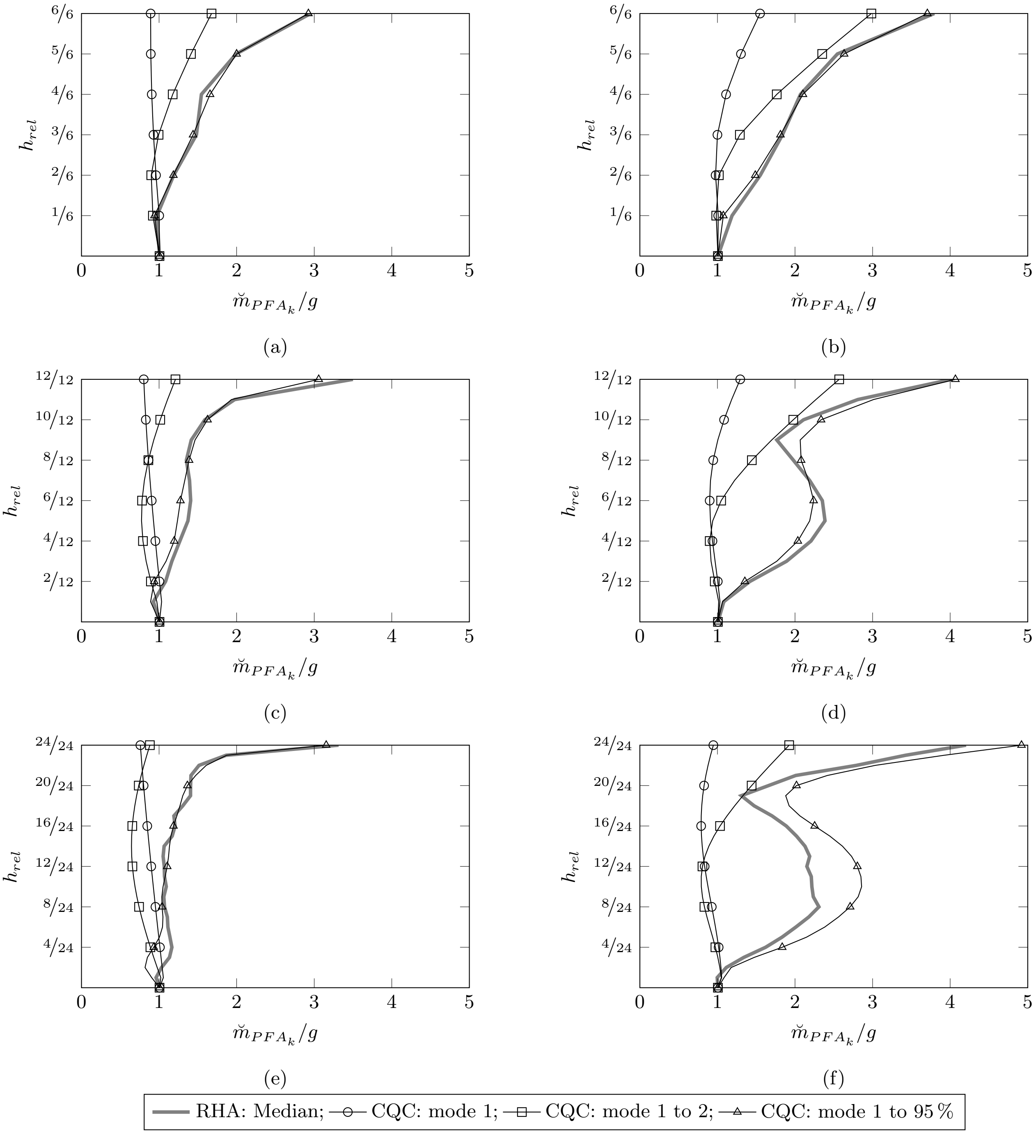


Figure 8: Median PFA demand profiles of a six-story (first row), a twelve-story (second row), and a 24-story (third row) spatial SMRF (left column) respectively structural WALL (right column). RHA benchmark solution and outcomes of the CQC modal combination rule based on one mode, two modes, and 95 % cumulative mass participating modes, respectively.

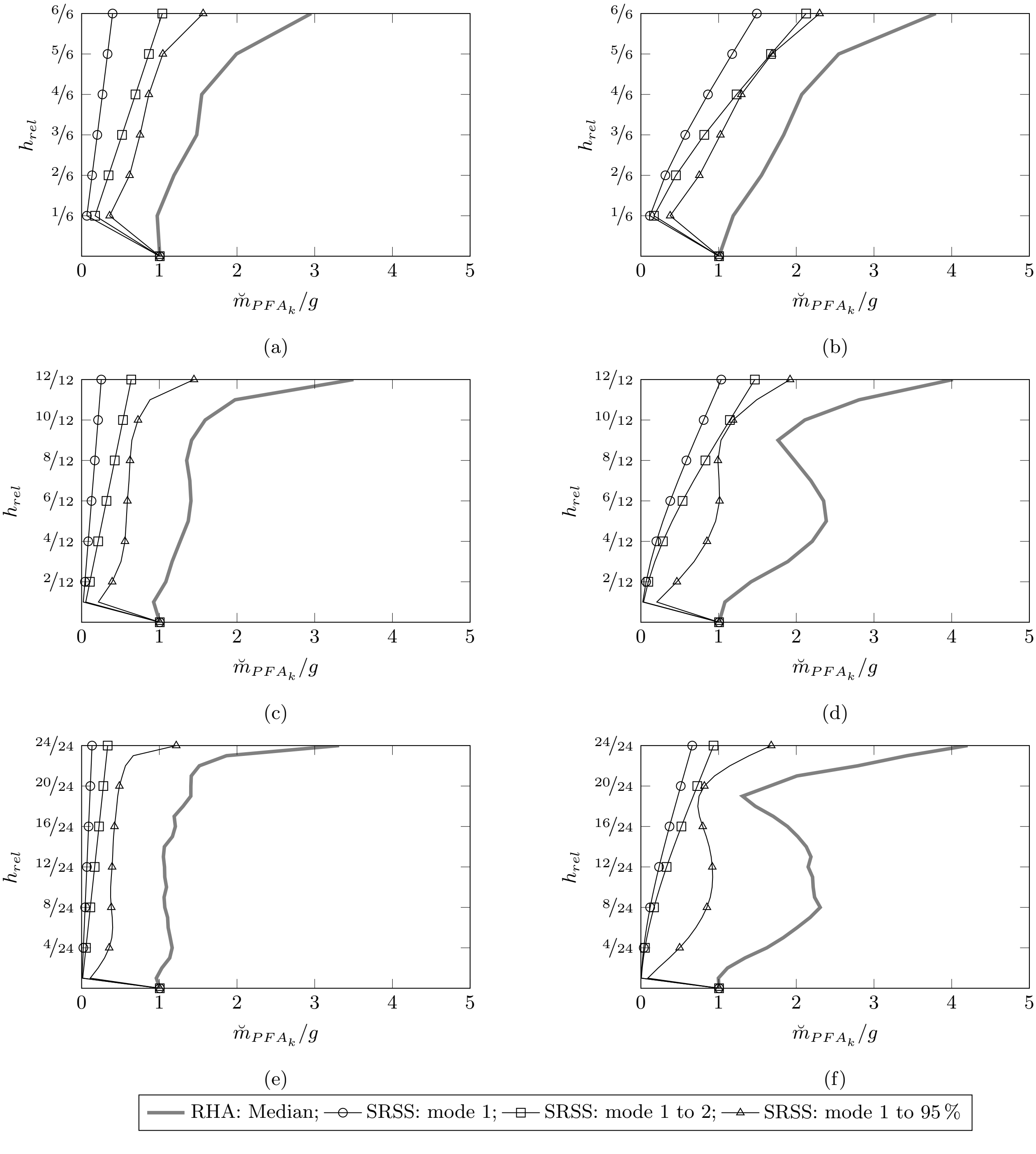


Figure 9: Median PFA demand profiles of a six-story (first row), a twelve-story (second row), and a 24-story (third row) spatial SMRF (left column) respectively structural WALL (right column). RHA benchmark solution and outcomes of the common SRSS modal combination rule based on one mode, two modes, and 95 % cumulative mass participating modes, respectively.

## 7. Summary, conclusions, and outlook

A closed form solution of a modal complete quadratic combination (CQC) rule for estimating seismic peak floor acceleration (PFA) demands in elastic structures has been proposed. The derivation has been shown in detail, beginning with modal response history analysis, and subsequent transition to random vibration theory, specialized to normal stationary processes of absolute accelerations. A rigorous analytical derivation has been presented for the first three cross-spectral moments of response processes based on the Kanai-Tajimi power spectral density. In contrast to existing CQC rules based on numerical approximations, closed form solutions for the correlation coefficients and an analytical approximation of the peak factors for the CQC rule have been derived. These analytical representations provide new insights into the correlation and statistics of peak acceleration response, offering a valid fully analytical counterpart to the original CQC method. The method has been applied to various planar and spatial generic structures subjected to a set of recorded ground motions, which match the design response spectrum of Century City, LA, *and* a given target dispersion. The outcomes have been validated with median PFA demands obtained from “exact” response history analysis and traditional modal combination rules. From these results it can be concluded that the proposed CQC rule closely approximates the median PFA demands of *elastic* structures, and thus, represents a significant enhancement of the state of the art of modal combination rules.

The application of the proposed approach within the PBEE framework, however, requires the approximation of fragility curves, i.e., the conditional cumulative distribution function $P\left[PFA \geq pfa|IM = im\right]$. This involves the prediction of *inelastic* PFA demands, which is still a challenging task. Generally, nonlinear dynamic methods and nonlinear static methods in terms of static pushover analysis are widely accepted to estimate the seismic demand of structures responding inelastically. Static approaches are computationally more efficient than dynamic ones, and thus generally preferred by engineers. Still they cannot provide PFA information. Interestingly enough, though, PFA demands are essentially strength controlled quantities that quickly saturate when a structure enters the inelastic range. Thus, for instance, FEMA P-58-1 [1] can offer generic modification factors that translate elastic to inelastic PFA demands, given the lateral strength ratio. When applying such procedures the bottleneck has been the estimation of elastic demands. The present contribution solves exactly this problem offering a firm basis for the inelastic PFA assessment.

## 8. Appendix: Required functions and functionals

### *8.1. Functionals in the denominators of the cross-spectral moments*

The functionals $D_1$, $D_2$, $D_3$, and $D_4$ in the denominators of the cross-spectral moments given by Equations (31) to (33) can be expressed as

$$\begin{aligned} D_1 &= K(\omega_g, \zeta_g, \omega_i, \zeta_i)K(\omega_g, \zeta_g, -\omega_i, \zeta_i)K(\omega_i, \zeta_i, -\omega_j, \zeta_j) \\ D_2 &= K(\omega_g, \zeta_g, \omega_j, \zeta_j)K(\omega_g, \zeta_g, -\omega_j, \zeta_j)K(\omega_i, \zeta_i, -\omega_j, \zeta_j) \\ D_3 &= K(\omega_g, \zeta_g, -\omega_i, \zeta_i)K(\omega_g, \zeta_g, \omega_j, \zeta_j) \\ D_4 &= K(\omega_g, \zeta_g, \omega_i, \zeta_i)K(\omega_g, \zeta_g, -\omega_j, \zeta_j) \end{aligned} \tag{35}$$

with

$$\begin{aligned} K(\omega_m, \zeta_m, \omega_n, \zeta_n) = {} & \left(\omega_m^2 - \omega_n^2\right)^2 \\ & + 4\omega_m\omega_n\left(-\omega_m^2\zeta_m\zeta_n + \omega_m\omega_n\zeta_m^2 + \omega_m\omega_n\zeta_n^2 - \omega_n^2\zeta_m\zeta_n\right) \end{aligned} \tag{36}$$

Here, subscripts $m, n = i, j, g$ indicate the $i$th mode, the $j$th mode, and the ground motion $g$ (for consistent notation, if $m, n = g$ then $\omega_g \equiv \nu_g$).

### *8.2. Recursion equations for the zeroth and the second cross-spectral moment*

The recursion equations for the functions in the zeroth and the second spectral moment are derived as

$$\begin{aligned} \xi_{l,mn}(\omega_i, \omega_j) &= \begin{cases} -\xi_{1,mn}(\omega_i, \omega_j) - 2\mathbb{i}^l\zeta_g\hat{\xi}_{1,mn}(\omega_i, \omega_j) & \text{if } m+n \text{ is even,} \\ +\xi_{1,mn}(\omega_i, \omega_j) - 2\mathbb{i}^l\zeta_g\hat{\xi}_{1,mn}(\omega_i, \omega_j) & \text{if } m+n \text{ is odd.} \end{cases} \\ \psi_{0,mn}(\omega_i, \omega_j) &= \begin{cases} \dfrac{\psi_{1,mn}(\omega_i, \omega_j)}{2} & \text{if } m = 0, \\ \dfrac{\psi_{1,mn}(\omega_i, \omega_j) - \hat{\psi}_{1,\overline{m}n}(\omega_i, \omega_j)}{2} & \text{if } m > 0. \end{cases} \\ \psi_{2,mn}(\omega_i, \omega_j) &= \begin{cases} \psi_{1,mn}(\omega_i, \omega_j) & \text{if } m > 4, \\ \psi_{1,mn}(\omega_i, \omega_j) - \psi_{0,mn}(\omega_i, \omega_j) & \text{otherwise.} \end{cases} \end{aligned} \tag{37}$$

in which subscript $\overline{m} = m - 1$, and $l = 1, 2$.

### *8.3. Functionals for the first cross-spectral moment*

The functionals in the first cross-spectral moment read as

$$\begin{aligned} &\xi_{1,01}(\omega_i, \omega_j) = -\xi_{1,10}(\omega_j, \omega_i) && \xi_{1,02}(\omega_i, \omega_j) = \xi_{1,20}(\omega_j, \omega_i) \\ &\xi_{1,12}(\omega_i, \omega_j) = -\xi_{1,21}(\omega_j, \omega_i) && \hat{\xi}_{1,01}(\omega_i, \omega_j) = -\hat{\xi}_{1,10}(\omega_j, \omega_i) \\ &\hat{\xi}_{1,02}(\omega_i, \omega_j) = \hat{\xi}_{1,20}(\omega_j, \omega_i) && \hat{\xi}_{1,12}(\omega_i, \omega_j) = -\hat{\xi}_{1,21}(\omega_j, \omega_i) \end{aligned} \tag{38}$$

Note that the off-diagonal elements of $\mathbf{\Xi}_1$ and $\hat{\mathbf{\Xi}}_1$ are determined by considering the sign and changing the frequencies $\omega_i$ and $\omega_j$ of their off-diagonal counterpart. All other elements of $\mathbf{\Xi}_1$ and $\hat{\mathbf{\Xi}}_1$ can be express in terms of the functionals

$$
\begin{aligned}
\xi_{1,00}(\omega_i,\omega_j) &= \omega_i\omega_j\left(\nu_g^2 X\left(\omega_j,\varphi_3',-\varphi_2\right)+\omega_i^2 X\left(\omega_j,-\varphi_1,\varphi_3'\right)\right)\\
\xi_{1,01}(\omega_i,\omega_j) &= 2\omega_i\nu_g\zeta_g\left(-\nu_g^2 X\left(\omega_j,2\varphi_3',3\right)+\omega_i^2 X\left(\omega_j,2\varphi_1,\varphi_2\right)\right)\\
\xi_{1,02}(\omega_i,\omega_j) &= 4\omega_i\omega_j\nu_g^2 X\left(\omega_i,-\varphi_1,\varphi_3'\right)\\
\xi_{1,11}(\omega_i,\omega_j) &= -4\varphi_3'\nu_g^6+16\varphi_1\omega_i^2\omega_j^2\nu_g^2\zeta_g^2+8\varphi_2\nu_g^4\zeta_g^2\left(\omega_i^2+\omega_j^2\right)\\
\xi_{1,12}(\omega_i,\omega_j) &= -8\omega_j\nu_g^3\zeta_g X\left(\omega_i,2\varphi_1,\varphi_2\right)\\
\xi_{1,22}(\omega_i,\omega_j) &= -16\varphi_1\omega_i\omega_j\nu_g^4\\
\hat{\xi}_{1,00}(\omega_i,\omega_j) &= -\omega_i\omega_j\zeta_g\left(\nu_g^2 X\left(\omega_j,1,-2\right)+\omega_i^2 X\left(\omega_j,4\zeta_g^2,1\right)\right)\\
\hat{\xi}_{1,01}(\omega_i,\omega_j) &= \omega_i\nu_g\left(\nu_g^2 X\left(\omega_j,-4\zeta_g^2,1\right)-\omega_i^2 X\left(\omega_j,\left(4\zeta_g^2\right)^2,\varphi_2'\right)\right)\\
\hat{\xi}_{1,02}(\omega_i,\omega_j) &= -4\omega_i\omega_j\nu_g^2\zeta_g X\left(\omega_i,4\zeta_g^2,1\right)\\
\hat{\xi}_{1,11}(\omega_i,\omega_j) &= 4\nu_g^2\zeta_g\left(\nu_g^2 X\left(\omega_j,\varphi_2',1\right)+\omega_i^2 X\left(\omega_j,\left(4\zeta_g^2\right)^2,\varphi_2'\right)\right)\\
\hat{\xi}_{1,12}(\omega_i,\omega_j) &= 4\omega_j\nu_g^3 X\left(\omega_i,\left(4\zeta_g^2\right)^2,\varphi_2'\right)\\
\hat{\xi}_{1,22}(\omega_i,\omega_j) &= -64\omega_i\omega_j\nu_g^4\zeta_g^3
\end{aligned}
\tag{39}
$$

For the elements of the matrices $\mathbf{\Psi}_1$ and $\hat{\mathbf{\Psi}}_1$ holds

$$
\begin{aligned}
\psi_{1,mn} &= 0 \quad \text{if } m+n \text{ is even}\\
\hat{\psi}_{1,mn} &= 0 \quad \text{if } m+n \text{ is odd}
\end{aligned}
\tag{40}
$$

The remaining elements of $\mathbf{\Psi}_1$ and $\hat{\mathbf{\Psi}}_1$ can be expressed in terms of the functionals

$$
\begin{aligned}
\psi_{1,01} &= 2\omega_i^3\hat{Y}_1(\omega_i) & \hat{\psi}_{1,00} &= \omega_j\left(\omega_j^2-\omega_i^2\right)\hat{Y}_1(\omega_i)\\
\psi_{1,10} &= \omega_j\left(\omega_j^2 Y_1(\omega_i)+Y_2(\omega_i)\right) & \hat{\psi}_{1,02} &= 4\omega_i^2\omega_j\hat{Y}_1(\omega_i)\\
\psi_{1,12} &= 4\omega_i^2\omega_j Y_1(\omega_i) & \hat{\psi}_{1,11} &= 4\omega_i\left(\omega_j^2\hat{Y}_1(\omega_i)+\hat{Y}_2(\omega_i)\right)\\
\psi_{1,21} &= 4\omega_i\left(\omega_j^2 Y_1(\omega_i)-Y_3(\omega_i)\right) & \hat{\psi}_{1,20} &= \psi_{1,30}+\frac{\psi_{1,50}}{2}+8\omega_i^6\omega_j\nu_g^2\\
\psi_{1,30} &= 4\omega_j\nu_g^2\left(\omega_j^2 Y_4(\omega_i)+4\omega_i^4\nu_g^2\zeta_g^2-\omega_i^6\right) & \hat{\psi}_{1,22} &= \psi_{1,32}+\frac{\psi_{1,52}}{2}\\
\psi_{1,32} &= 16\omega_i^2\omega_j\nu_g^2 Y_4(\omega_i) & \hat{\psi}_{1,31} &= \psi_{1,41}+\frac{\psi_{1,61}}{2}\\
\psi_{1,41} &= 16\omega_i\nu_g^2\left(\omega_j^2 Y_4(\omega_i)+4\omega_i^4\nu_g^2\zeta_g^2\right) & \hat{\psi}_{1,40} &= \psi_{1,50}\\
\psi_{1,50} &= 64\omega_i^2\omega_j^3\nu_g^4\zeta_g^2 & \hat{\psi}_{1,42} &= \psi_{1,52}\\
\psi_{1,52} &= 256\omega_i^4\omega_j\nu_g^4\zeta_g^2 & \hat{\psi}_{1,51} &= \psi_{1,61}\\
\psi_{1,61} &= 256\omega_i^3\omega_j^2\nu_g^4\zeta_g^2 & &
\end{aligned}
\tag{41}
$$

where the required functions read as

$$\begin{aligned}
&\varphi_1 = 1 + 4\zeta_g^2 - 8\zeta_g^4 && \varphi_4 = 1 - 12\zeta_g^2 && \varphi_2' = 1 + 4\zeta_g^2 \\
&\varphi_2 = 1 - 4\zeta_g^2 && \varphi_5 = 1 + 24\zeta_g^2 - 48\zeta_g^4 && \varphi_3' = 1 + 2\zeta_g^2 \\
&\varphi_3 = 1 - 2\zeta_g^2
\end{aligned} \tag{42}$$

$$X(\omega_i, a, b) = a\omega_i^2 + b\nu_g^2$$

$$\begin{aligned}
Y_1(\omega_i) &= -\varphi_5\omega_i^4\nu_g^2 - 2\varphi_4\omega_i^2\nu_g^4 + 3\nu_g^6 + 4\omega_i^6\zeta_g^2 \\
Y_2(\omega_i) &= \omega_i^2\nu_g^2\left(3\omega_i^4 - \nu_g^4 + 2\omega_i^2\left(4\varphi_3\omega_i^2\zeta_g^2 - \varphi_2'\nu_g^2\right)\right) + 4\omega_i^8\zeta_g^2 \\
Y_3(\omega_i) &= \omega_i^2\nu_g^2\left(\omega_i^2\left(16\nu_g^2\zeta_g^2 + \varphi_2^2\omega_i^2\right) + \nu_g^4\right) \\
Y_4(\omega_i) &= 8\varphi_3\omega_i^4\zeta_g^2 - \nu_g^4 - 20\omega_i^2\nu_g^2\zeta_g^2 \\
\hat{Y}_1(\omega_i) &= \varphi_2^2\omega_i^4\nu_g^2 - 2\varphi_2\omega_i^2\nu_g^4 + \nu_g^6 + 4\omega_i^6\zeta_g^2 \\
\hat{Y}_2(\omega_i) &= \omega_i^2\nu_g^2\left(\omega_i^4 - \nu_g^4 + 8\omega_i^2\zeta_g^2\left(\varphi_3\omega_i^2 - \nu_g^2\right)\right)
\end{aligned} \tag{43}$$


## Acknowledgments

L. Moschen conducted the research for this paper as student of the Doctoral School (FWF DK-PLUS) *Computational Interdisciplinary Modelling*, which is based at the University of Innsbruck, Austria, and substantially funded by the Austrian Science Fund (FWF). Additionally, this study was partially supported by the Austrian Ministry of Science BMWF as part of the *UniInfrastrukturprogramm* of the Focal Point Scientific Computing at the University of Innsbruck, Austria, and by the DAAD organization, Germany, through the project *DeGrie Lab-Hybrid and Virtual Experimentation for Infrastructures* (Grant No 57055451, directed by Aristotle University of Thessaloniki, Greece and the University of Weimar, Germany).


## References


[1] FEMA P-58-1, Seismic performance assessment of buildings, volume 1 – methodology (2012).

[2] ASCE/SEI 7-10, Minimum design loads for buildings and other structures (2010).

[3] R. S. Chaudhuri, T. C. Hutchinson, Distribution of peak horizontal floor acceleration for estimating nonstructural element vulnerability, in: Proceedings of the 13th World Conference on Earthquake Engineering (13WCEE), Vancouver, Canada, 2004.

[4] R. S. Chaudhuri, T. C. Hutchinson, Effect of nonlinearity of frame buildings on peak horizontal floor acceleration, Journal of Earthquake Engineering (1) (2011) 124–142.

[5] E. Rosenblueth, J. Elorduy, Response of linear systems to certain transient disturbances, in: Proceedings of the 4th World Conference on Earthquake Engineering (4WCEE), Santiago, Chile, 1969, pp. 185–196.

[6] S. H. Crandall, W. D. Mark, Random Vibration in Mechanical Systems, Academic Press Inc., 111 Fifth Avenue, New York 3, New York, 1963.

[7] A. Der Kiureghian, A response spectrum method for random vibrations, 1980, UCB/EERC Report 80/15.

[8] A. Der Kiureghian, On response of structures to stationary excitation, 1979, UCB/EERC Report 79/32.

[9] A. Der Kiureghian, Structural response to stationary excitation, Journal of the Engineering Mechanics Division (1980) 1195–1213.

[10] E. L. Wilson, A. Der Kiureghian, E. P. Bayo, A replacement for the SRSS method in seismic analysis, Earthquake Engineering & Structural Dynamics (2) (1981) 187–192.

[11] P. Cacciola, N. Maugeri, G. Muscolino, A modal correction method for non-stationary random vibrations of linear systems 22 (2007) 170–180. doi:10.1016/j.probengmech.2006.10.002.

[12] C. A. Schenk, H. J. Pradlwarter, G. I. Schuëller, Non-stationary response of large, non-linear finite element systems under stochastic loading 83 (2005) 1086–1102. doi:10.1016/j.compstruc.2004.11.018.

[13] S. Taghavi, E. Miranda, Response spectrum method for estimation of peak floor acceleration demand, in: Proceedings of the 14th World Conference on Earthquake Engineering (14WCEE), Beijing, China, 2008.

[14] S. Taghavi, Probabilistic seismic assessment of floor acceleration demands in multi-story buildings, Ph.D. thesis, Stanford University (2006).

[15] M. Pozzi, A. Der Kiureghian, Response spectrum analysis for floor acceleration, in: Proceedings of the 15th World Conference on Earthquake Engineering (15WCEE), Lisbon, Portugal, 2012.

[16] M. Pozzi, A. Der Kiureghian, Response spectrum analysis for floor acceleration, Earthquake Engineering & Structural Dynamics (12) (2015) 2111–2127.

[17] A. K. Chopra, Dynamics of Structures: Theory and Applications to Earthquake Engineering, Prentice Hall, Boston, 2012.

[18] A. Der Kiureghian, Y. Nakamura, CQC modal combination rule for high-frequency modes, Earthquake Engineering & Structural Dynamics (11) (1993) 943–956.

[19] K. Kanai, Semi-empirical formula for the seismic characteristics of the ground, Bulletin of the Earthquake Research Institute (1957) 309–325.

[20] H. Tajimi, A statistical method of determining the maximum response of a building structure during an earthquake, in: Proceedings of the 2nd World Conference on Earthquake Engineering (2WCEE), Tokyo and Kyoto, Japan, 1960, pp. 781–797.

[21] H. Thráinsson, Modeling of earthquake ground motion in the frequency domain, Ph.D. thesis, Stanford University (2000).

[22] P. Spanos, L. V. Loli, A statistical approach to generation of design spectrum compatible earthquake time histories, International Journal of Soil Dynamics and Earthquake Engineering 4 (1) (1985) 2 – 8.

[23] A. Giaralis, P. Spanos, Wavelet-based response spectrum compatible synthesis of accelerogramseurocode application (ec8), Soil Dynamics and Earthquake Engineering 29 (1) (2009) 219 – 235.

[24] European Committee for Standardization, Eurocode 8: Design of structures for earthquake resistance - part 1: General rules, seismic actions and rules for buildings (2013).

[25] Pacific Earthquake Engineering Research Center, PEER ground motion database (2010).

[26] L. Moschen, R. A. Medina, C. Adam, A ground motion record selection approach based on multi-objective optimization (2015) In Preparation.

[27] E. Vanmarcke, Random Fields: Analysis and Synthesis, World Scientific, Singapore and Hackensack, NJ, 2010.

[28] A. Der Kiureghian, A response spectrum method for random vibration analysis of mdf systems, Earthquake Engineering & Structural Dynamics (5) (1981) 419–435.

[29] E. H. Vanmarcke, On the distribution of the first-passage time for normal stationary random processes, Journal of Applied Mechanics (1) (1975) 215–220.

[30] W. Feller, An Introduction to Probability Theory and its Applications, Wiley Series in Probability and Mathematical Statistics, Wiley, New York, 1968.

[31] J. R. Benjamin, C. A. Cornell, Probability, Statistics, and Decision for Civil Engineers, Dover Publications, 1970.

[32] N. Wiener, Generalized harmonic analysis, Acta Mathematica (1930) 117–258.

[33] A. Khintchine, Korrelationstheorie der stationären stochastischen prozesse (in German), Mathematische Annalen (1934) 604–615.

[34] A. V. Oppenheim, R. W. Schafer, J. R. Buck, Discrete-time signal processing, 2nd Edition, Prentice Hall signal processing series, Prentice Hall, 1999.

[35] R. N. Bracewell, The Fourier Transform and its Applications, 3rd Edition, McGraw-Hill series in electrical and computer engineering. Circuits and systems, McGraw Hill, 2000.

[36] N. Shome, C. A. Cornell, P. Bazzurro, J. E. Carballo, Earthquakes, records, and nonlinear responses, Earthquake Spectra (3) (1998) 469–500.

[37] N. Shome, C. A. Cornell, P. Bazzurro, J. E. Carballo, Earthquakes, records and nonlinear mdof responses: Rms report no. 29, 1997, reliability of Marine Structures Program.

[38] S. H. Crandall, First-crossing probabilities of the linear oscillator, Journal of Sound and Vibration (3) (1970) 285–299.

[39] S. H. Crandall, K. L. Chandiramani, R. G. Cook, Some first-passage problems in random vibration, Journal of Applied Mechanics (3).

[40] M. Shinozuka, W. F. Wu, On the first passage problem and its application to earthquake engineering, in: Proceedings of the 9th World Conference on Earthquake Engineering (9WCEE), Tokyo, Japan, 1988, pp. 767–772.

[41] S. O. Rice, Mathematical analysis of random noise, Bell System Technical Journal (3) (1944) 282–332.

[42] E. H. Vanmarcke, Properties of spectral moments with appilcations to random vibration, Journal of the Engineering Mechanics Division (1972) 425–446.

[43] N. Shome, Probabilistic seismic demand analysis of nonlinear structures, Ph.D. thesis, Stanford University (1999).

[44] M. Dresher, The Mathematics of Games of Strategy: Theory and Applications, Dover, New York, 1981.

[45] L. Moschen, Contributions to the probabilistic seismic assessment of acceleration demands in buildings, Ph.D. thesis, University of Innsbruck, Innsbruck Austria (2016).

[46] R. A. Medina, Seismic demands for nondeteriorating frame structures and their dependence on ground motions, Ph.D. thesis, Stanford University (2003).